J Low Temp Phys (2013) 171:178–186
DOI 10.1007/s10909-012-0712-6

Experimental Investigation of Exotic Negative Ions in Superfluid Helium

W. Wei · Z.-L. Xie · G.M. Seidel · H.J. Maris

Received: 3 July 2012 / Accepted: 24 August 2012 / Published online: 6 September 2012
© Springer Science+Business Media, LLC 2012

Abstract We have constructed a new apparatus designed to study the exotic negative ions in superfluid helium-4 previously observed. Our apparatus is similar to that used by Ihas and Sanders, and by Eden and McClintock. The ions are generated from an electrical discharge in the vapor above the surface of the liquid and the mobility is measured by the time-of-flight method. We have detected eleven exotic ions with distinct mobility, and have measured their mobility as a function of temperature. In addition to the peaks in the time-of-flight signal due to the different exotic ions, there is a smoothly varying and continuous background signal. The variation of the background with field and temperature appears to be inconsistent with any explanation invoking the decay of one exotic ion into another, and supports the idea it arises from negative ions with a continuous distribution of mobility. This is a striking result because it would indicate that these ions have a continuous size distribution.

Keywords Exotic ions · Mobility · Time-of-flight

1 Introduction

There have been a large number of studies of both negative and positive ions in liquid helium. For positive ions the results support the "snowball" model, i.e., a small spherical volume of solid surrounding the ionized helium atom [1]. The normal negative ion consists of an electron confined in a bubble of radius about 19 Å which is free of helium atoms [2]. However, in addition to these well studied objects, other ions have been detected. Doake and Gribbon [3] detected a "fast ion" with a mobility about seven times that of the normal negative ion. Ihas and Sanders [4–6] confirmed the existence of this ion and then discovered twelve more objects with mobility between

W. Wei (✉) · Z.-L. Xie · G.M. Seidel · H.J. Maris
Department of Physics, Brown University, Providence, RI 02912, USA
e-mail: Wanchun_Wei@brown.edu

that of the fast ion and the mobility of the normal ion. McClintock and coworkers made further studies of these ions, and were able to determine the critical velocity at which quantized vortices were nucleated [7–9].

The higher mobility of the ions implies that they are smaller than normal ions. Based on the assumptions that the mobility is limited by interaction of the ions with rotons and varies as the inverse square of the ion radius, the radius R is estimated to vary from about 8 Å for the fast ion up to a value of around 90 % of the radius of the normal ion for the slowest of the exotic ions. Ihas [6] has discussed a number of possible models for the exotic ions and has concluded that none of them can explain the experimental data. In this contribution we report on the construction of a new apparatus to study these objects, describe some of the results that have been obtained, and comment on the implications of these results.

2 Experiment

In the experiments to study the exotic ions by Ihas and Sanders [4–6] and by Eden and McClintock [7–9] the ions entered the liquid from a plasma formed in the helium vapor above the liquid surface. The electrical discharge resulted in a substantial heat input, and in order to maintain the temperature at around 1 K it was necessary to use a powerful pumping system. In the earlier experiments this problem was solved by using a large pump to pump directly on the main helium bath. This method has the disadvantage that the experiment has to be stopped periodically so that the bath can be refilled. To avoid this problem, we have constructed an apparatus with an especially-designed 1 K pot which enables us to operate continuously at temperatures below 1 K even with a dissipation of 50 mW in the plasma. We have used an Edwards EH1200 Roots pump with backing from an Alcatel 2063H. A helium-4 pot is preferred over a helium-3 pot for this application because of the larger latent heat of evaporation. The experimental cell is bolted directly to the 1 K pot with heat transfer across an oxygen-free copper plate.

As shown in Fig. 1, the design of our cell is very similar to that of Ihas and Sanders, and Eden and McClintock. A discharge is produced between the tungsten tips T and the plate P. This plate contains a number of holes to allow ions to pass through; the size and arrangement of these holes was different in different experimental runs. The gate grid G2 is normally held at a potential negative with respect to gate G1, thereby preventing negatively-charged ions passing into the drift region below G2. By applying a negative voltage pulse to G1 a pulse of ions is allowed to pass through G2 into the drift region. The length of this region is 6.15 cm. The drift region includes four field homogenizer disks (plates with a 1.27 cm diameter hole) held at potentials appropriate for maintaining the electric field as uniform as possible throughout the drift region. However, ions passing close to the edge of the hole will experience a non-uniform field with consequences discussed below.

There are a large number of experimental parameters which can be varied. In addition to the voltages on the different electrodes and the plate geometry, the number, arrangement and sharpness of the tungsten tips affect the discharge. The discharge is also greatly affected by the density of the helium vapor which around 1 K varies rapidly with temperature.

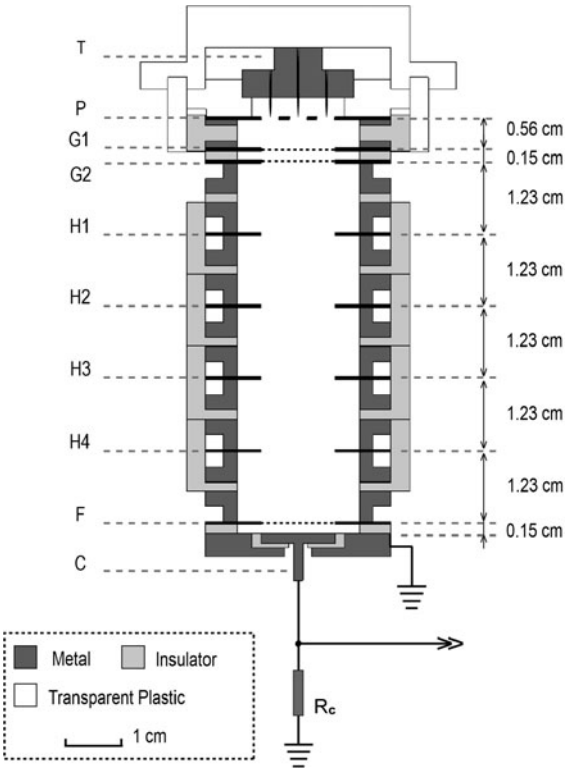

Fig. 1 Cross-section of the experimental cell showing the tungsten tips T, the perforated plate P, the gate grids G1 and G2, the field homogenizers H1, H2, H3, and H4, the Frisch grid F and the collector C

After moving through the drift region the ions pass through a Frisch grid F and reach the collector C. The ion current passes to ground through the load resistor R_c of 2.46 MΩ. The voltage across this resistor is measured using a Stanford Instruments SR560 amplifier. To keep the time resolution as good as possible we reduced the capacitance of the cable to the amplifier by bringing it out through the tail of the cryostat. To achieve a reasonable signal to noise ratio, we typically averaged 5,000 to 20,000 traces.

The cell was installed in a cryostat with optical access, making it possible to observe the discharge and analyze the spectrum of light emitted. We will describe more details of the apparatus, its operation, and results obtained in a subsequent publication.

3 Results

A representative dataset is shown in Fig. 2. This shows results taken at 0.991 K with a drift field of 82.1 $\mathrm{V\,cm^{-1}}$ and a 0.4 ms wide gate pulse. In this data set we can identify above the noise ten exotic ions in addition to the fast ion. Although the signal to noise is excellent, some details of the ions are obscured by the long tail extending after each ion peak. This tail arises from the time constant of the detection circuit (~ 0.25 ms) combined with the inhomogeneity of the drift field. Ions which pass

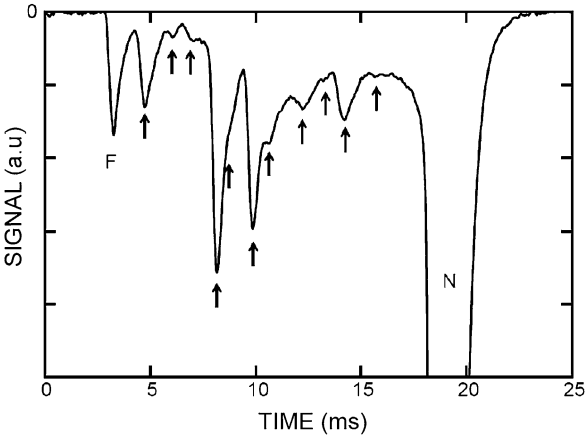

Fig. 2 Representative data set taken at 0.991 K with a drift field of 82.1 V cm^{-1} and a 0.4 ms wide gate pulse. F denotes the fast ion, N the normal negative ion, and the *arrows* indicate the time of arrival of eleven of the exotic ions

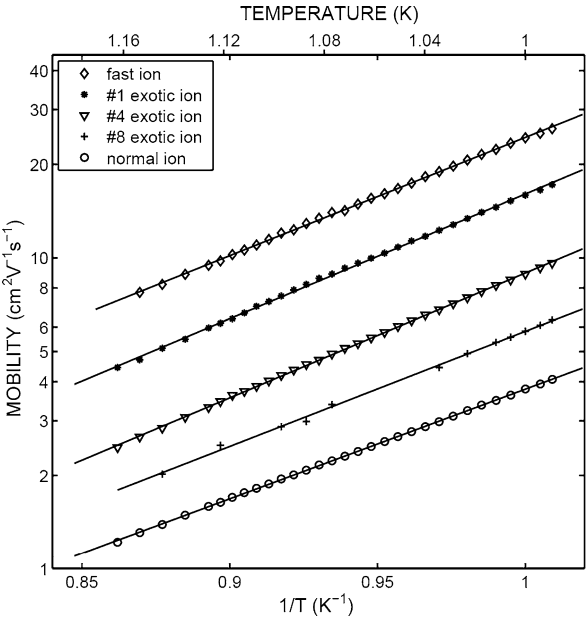

Fig. 3 Mobility of the ions as a function of temperature

close to the edge of the holes in the field homogenizers have a longer transit time than ions moving along the axis of the cell. From data of the type shown in Fig. 2 we can measure the mobility of each ion as a function of temperature and results are shown in Fig. 3. These results are in reasonable agreement with the results obtained by Ihas and Sanders. The mobilities we measure are typically 5 % lower than the results of Ihas and Sanders; the difference increases to almost 20 % at the lowest temperature. These differences are probably caused by a small error in the temperature calibration and difficulty in determining the effective length of the cell. Nevertheless, through the measured mobility we have been able to identify each ion with one of the ions observed by Ihas and Sanders.

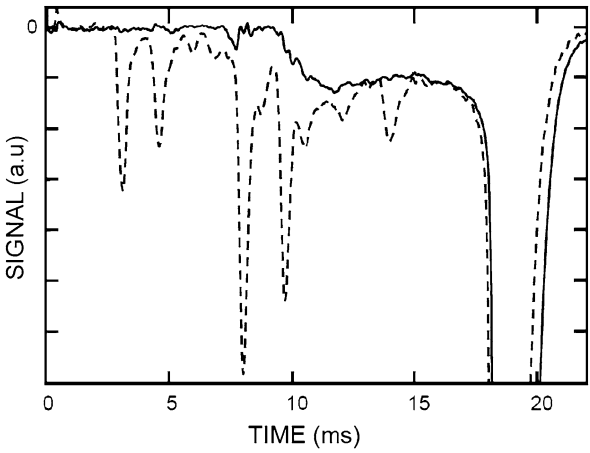

Fig. 4 *Solid curve* shows the mobility data of Fig. 2 with the peaks due to exotic ions removed as described in the text. The *dashed curve* shows the data of Fig. 2 processed so as to sharpen the peaks due to the exotic ions

A detailed examination of the signal traces as a function of time reveals that in addition to the peaks coming from the exotic ions, there is a continuously-varying background. To view this background we have to remove the peaks. This cannot be done in a completely rigorous way since we do not have a way to determine the peak shape, particularly the tail. In Fig. 4 we show the results of two attempts at solving this problem. We use the same data set as shown in Fig. 2.

(1) In the first attempt, we have estimated the background by removing the peaks. We approximated the shape of each peak by a function $g(t)$ given by

$$g(t) = Af(t - t_{\text{start}}) \exp\left[-(t - t_{\text{start}})/t_{\text{fall}}\right] \tag{1}$$

with

$$f(t) = \begin{cases} 0 & t < 0 \\ t^2 - t^6/3t_{\text{rise}}^4 & 0 < t < t_{\text{rise}} \\ 2t_{\text{rise}}^2/3 & t > t_{\text{rise}} \end{cases} \tag{2}$$

where $A, t_{\text{start}}, t_{\text{rise}}$, and t_{fall} are coefficients chosen for each peak. We have subtracted a series of functions of this form from the data, choosing these parameters so as to minimize any obvious sign of each peak. The result is shown as the solid line.

(2) In the second approach we sharpen each peak (as distinct from removing it) so as to make it easier to distinguish between peaks and background. This is based on the following model. The broadening of each peak is caused in part by the effect of the stray capacitance C. If this is the only cause of broadening, the relation between the actual measured signal $\tilde{S}(t)$ and the signal $S(t)$ in the absence of any capacitance would be

$$S(t) = \tilde{S}(t) + \tau \frac{d\tilde{S}}{dt}, \tag{3}$$

where $\tau = R_c C = 0.26$ ms. The result is shown by the dashed line in Fig. 4. One can see that this procedure gives a significant narrowing of the peaks and makes it clearer that a background is indeed present.

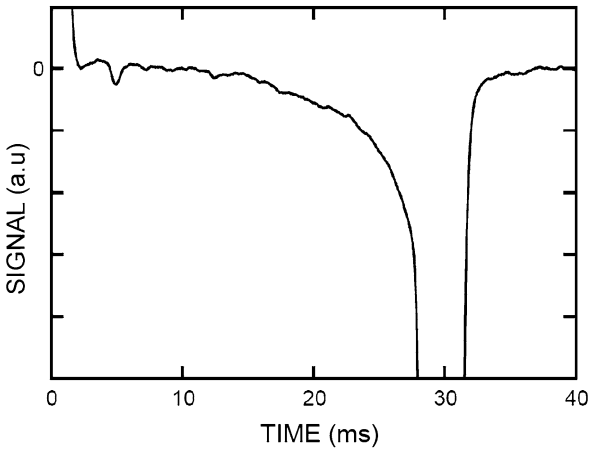

Fig. 5 An example of a signal obtained showing background of type #II. The temperature was 1.025 K, the drift field was 67.2 V cm^{-1}

From these procedures it is evident that there is a continuous background (CB) which starts at a time τ_B which is approximately half the arrival time of the normal ion pulse. In fact, earlier data of Ihas and Sanders[1] show a CB similar to the results shown in Fig. 4, although they did not make any comment concerning this.

The form of the background changes considerably when the characteristics of the discharge are changed, for example, by changing the voltages applied to the tip and the plate. We have even been able to find conditions such that a small change in the tip current switches the background from the form shown in Fig. 4 (type #I) to the form shown in Fig. 5 (type #II). The background (type #II) shown in Fig. 5 decreases steadily with decrease in t and it is not clear whether the background has a cut-off at some time or simply becomes too small to see in the presence of noise.

We have also investigated how the background changes with drift field and temperature. Data for different fields are shown in Fig. 6. In this data set, the exotic ions were weak, so that the continuous background (type #I) was clearly exposed without the need for mathematical subtraction of peaks. The continuous background shifts to earlier time when the drift field is increased; τ_B varies inversely with the drift field E. A corresponding shift occurs when the temperature is lowered. For type #II one can see from Fig. 6 that the background moves to earlier times as E increases, but since there is no sharp cut-off it is not possible to make a quantitative statement about how it varies with field.

4 Discussion

The existence of both types of continuous background is an important result and constitutes a major challenge to any theory of the exotic ions.

One possibility is that one or more of the faster exotic ions is unstable and decays into one or more of the slower ions. Suppose, for example, that ion m with mobility

[1] See Fig. 2 of [5].

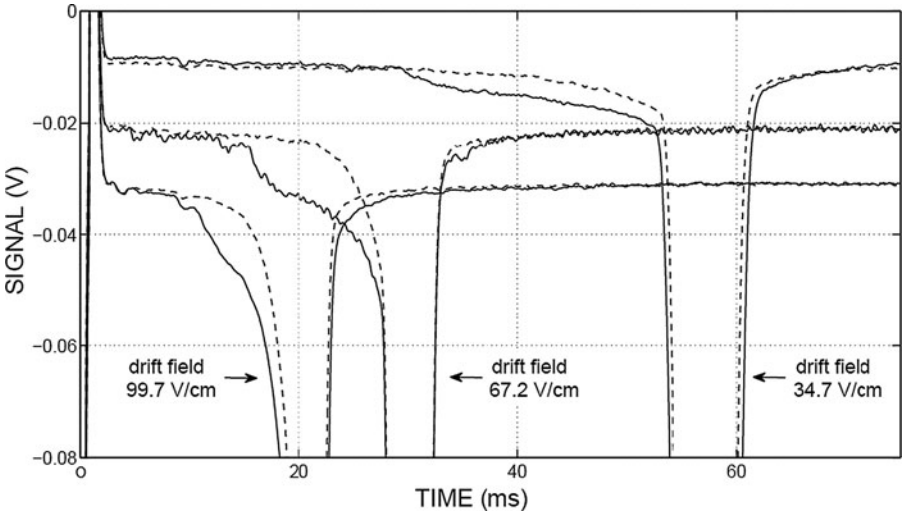

Fig. 6 Signals obtained for drift fields of 99.7, 67.2 and 34.7 V cm^{-1}. The temperature is 1.025 K

μ_m decays into a slower ion n with mobility μ_n, then the total current reaching the detector from ion m will be

$$I(t) = Ne\mu_m E\delta(d - \mu_m Et)\exp\left(-\frac{d}{\mu_m E\tau_m}\right) + \tilde{I}(t) \tag{4}$$

where N is the initial number of m ions, d is the length of the drift region, τ_m is the lifetime of ion m, E is the drift field, and $\tilde{I}(t)$ is the contribution from the ions which have decayed and is given by

$$\tilde{I}(t) = \frac{Ne}{\tau_m}\frac{\mu_n}{\mu_m - \mu_n}\exp\left[-\frac{d}{(\mu_m - \mu_n)E\tau_m}\right]\exp\left[\frac{\mu_n t}{(\mu_m - \mu_n)\tau_m}\right] \tag{5}$$

In order to have a background extending out to the arrival time of the normal ion, the decay product (ion n) has to be the normal ion. As far as we can see at the moment, Eqs. (4) and (5) do not give a good fit to the data, although it is conceivable that some combination of multiple decay steps could give a fit.

We also note that the proposal that the background comes from decay of one ion into another is inconsistent with the data shown in Fig. 6. The background would have a very different shape according to the relative magnitude of the decay time and the total transit time.

The more straightforward interpretation is that in addition to the eleven or so ions with discrete mobilities there are also ions which have a continuous distribution of mobility, and therefore, presumably have a continuous size distribution. Three very different possible theories of exotic ions have been discussed.

1. Impurities could be sputtered from the walls of the cell. In order for the ions, to be negative impurity ions there would have to be eleven different impurities of roughly equal concentration. Also the same impurities would need to be present in the cell used by Ihas and Sanders. This is unlikely. The electron affinity of each

one of these impurities would have to lie in the range required to give ions with the radius that is observed [10, 11]. A final difficulty is that it does not appear possible for impurities to explain the existence of the continuous background.

2. Ihas and Sanders [4, 6] have discussed the possibility that one or more of the exotic ions are helium negative ions with electron configuration $1s^{\uparrow}2s^{\uparrow}2p^{\uparrow}$. Of this multiplet of states, the one with the longest lifetime decays in 345 μs in vacuum. This is much less than the transit time in our experiment and so one would have to assume that for some reason the lifetime is increased for an ion in the liquid. Even if this increase in lifetime does occur, the helium negative ion would still provide an explanation for only one of the exotic ions and also would leave unresolved the origin of the background.
3. The final possibility to consider is the fission model [12]. In this model the key assumption is that it is possible for stable bubbles to exist which contain only a fraction of the wave function of an electron, i.e., bubbles in which the integral I of $|\psi|^2$ over the volume of the bubble is less than one. If it is accepted that such bubbles can be stable, there are at least three mechanisms by which they could be formed. The first mechanism is through optical excitation. After a normal electron bubble ($I = 1$) is excited to a higher energy state through absorption of a photon, the shape of the bubble changes and may evolve in a way such that the bubble breaks up into smaller bubbles.[2] The light emitted from the discharge in the vapor could cause this to happen. The second and third mechanisms concern the processes that take place when an electron enters the liquid from the discharge in the vapor. After an electron entering the liquid has lost most of its energy through collisions with helium atoms, the wave function will have a very complex form and may localize into more than one bubble. This could give rise to bubbles with a continuous distribution of I (and hence of size), and also certain discrete sizes could result. The third mechanism concerns what happens to an electron which has an energy only slightly above the height of the barrier against entry into the liquid (~ 1 eV). The wave packet representing such an electron will be only partially transmitted into the liquid, i.e., the integral of $|\psi|^2$ within the liquid will be less than one. It is natural to ask how such electrons form bubbles, and to consider the possibility that these electrons make a significant contribution to the continuous background.

We will give a full presentation of the experimental results and a more detailed discussion of their relation to theory in a subsequent paper.

Acknowledgements We thank Leon Cooper for many stimulating discussions concerning the interpretation of these results. This work was supported in part by the United States National Science Foundation under Grant No. DMR 0965728.

References

1. K.R. Atkins, Phys. Rev. **116**, 1339 (1959)

[2]For examples of calculations of this type, see [12–15].

2. R.A. Ferrell, Phys. Rev. **108**, 167 (1957)
3. C.S.M. Doake, P.W.F. Gribbon, Phys. Lett. A **30**, 251 (1969)
4. G.G. Ihas, T.M. Sanders, Phys. Rev. Lett. **27**, 383 (1971)
5. G.G. Ihas, T.M. Sanders, in *Proceedings of the 13th International Conference on Low Temperature Physics*, vol. 1, ed. by K.D. Timmerhaus, W.J. O'Sullivan, E.F. Hammel (Plenum, New York, 1972), p. 477
6. G.G. Ihas, Ph.D. thesis, University of Michigan (1971)
7. V.L. Eden, P.V.E. McClintock, in *The Proceedings of the 75th Jubilee Conference on Liquid Helium-4*, St. Andrews (1983)
8. V.L. Eden, P.V.E. McClintock, Phys. Lett. A **102**, 197 (1984)
9. C.D.H. Williams, P.C. Hendry, P.V.E. McClintock, Jpn. J. Appl. Phys. **26**(3), 105 (1987)
10. H.J. Maris, J. Phys. Soc. Jpn. **77**, 111008 (2008)
11. P.D. Grigorev, A.M. Dyugaev, Sov. Phys. JETP **88**, 325 (1999)
12. H.J. Maris, J. Low Temp. Phys. **120**, 173 (2000)
13. D. Mateo, M. Pi, M. Barranco, Phys. Rev. B **81**, 174510 (2010)
14. D. Mateo, D. Jin, M. Barranco, M. Pi, J. Chem. Phys. **134**, 044507 (2011)
15. D. Jin, W. Guo, W. Wei, H.J. Maris, J. Low Temp. Phys. **158**, 307 (2010)